

Developing High-Brightness Electron Beam Sources for Producing
Quantum Degenerate Electron Beams

By
Jonathan Kohler

Senior Honors Thesis

Submitted to the Faculty of the
Department of Physics and Astronomy
of
Vanderbilt University
in partial fulfillment of the requirements for
DEPARTMENTAL HONORS
in
Physics
Spring 2011

Advisor: Charles A. Brau

Faculty Committee:

Richard F. Haglund

Kalman Varga

Kenneth E. Schriver

1 Abstract

The Pauli Exclusion Principle places a fundamental limit on the brightness of an electron beam. Developing a cathode which can reach this limit is useful for achieving maximum operation in current applications of electron beams, but also opens new areas of physics to be explored. When the phase space of the electron beam is filled to the maximum density, the electrons will experience a degeneracy pressure, similar to that which keeps a neutron star from collapsing. One promising source for a quantum degenerate beam is field emission from adsorbates on carbon nanotubes. Adsorbates have been shown to provide several orders of magnitude enhancement to emission brightness, which approaches the degeneracy limit. We have developed experiments to test various adsorbates, in order to find those which bind tightest and provide the largest enhancement in brightness. Continuing work to discover better adsorbates should soon allow for the generation of a quantum degenerate electron beam.

2 Motivation & Previous Work

Since their discovery, carbon nanotubes (CNTs) have been the center of much research, due to their novel properties. While widespread commercial applications remain on the horizon, they hold clues to new phenomena which, once understood, could lead to significant applications. Because of the wide range of parameters describing their structure, the variations in the electronic structures of CNTs has received extensive research, in hopes of developing the ability to design systems with known electronic behavior as an alternative to traditional semiconductors. But their high electrical conductivity, thermal resistance, and chemical stability make them useful for many other applications.

It is well known that CNTs function well as electron field-emitters, due to their high aspect ratio. Electron-beam cathodes are important in areas from particle accelerators and free electron lasers to electron microscopy. CNTs offer several benefits compared to traditional cathodes. Thermionic emitters are widely used, but have low current density and therefore low brightness. Photoelectric sources provide more control over emission properties, but require large, complicated laser systems to operate. Field-emission sources offer a simpler mechanism, which can be easily controlled just using the electric field, but traditional field-emission cathodes, such as tungsten needles, are very noisy.

Nanotubes, including CNTs as well as boron nitride nanotubes (BNNTs), are unique as field emitters. Due to their high structural and thermal strength, they can withstand large emission currents, and their rigid structure and low chemical reactivity make them very stable sources of emission current. Since field emission is strongly dependent on electric field strength, emission is strongest at points of high curvature on the CNT cap, where the field enhancement factor is greatest. This produces very intense, localized emission with a spectrum describe by the Fowler-Nordheim equations [1]. The combination of large currents and the small source size and energy distribution creates one of the brightest electron

sources available. Since the phase-space density of an electron beam is conserved, due to Liouville's theorem, the brightness of a beam is determined by the cathode and cannot be improved by focusing, so high-brightness sources are applicable in any current application requiring intense electron beams.

The brightness of an electron beam is given by

$$B_N = m_e^2 c^2 \frac{d^4 I_e}{dx dp_x dy dp_y}$$

where I_e is the emission current. Due to the Pauli exclusion principle, there is a maximum brightness theoretically achievable by an electron beam, as the 6-dimensional phase space density is fundamentally limited, with one electron spin up-down pair in each h^3 unit of phase space volume. This brightness sets a limit on all current devices relying on high brightness sources, but also introduces new properties due to the degeneracy pressure introduced in the beam. The quantum degeneracy, ranging from 0-1, is given by [2]

$$\delta = \frac{h^3}{2m^2 c^2 q^2} \frac{B_N}{\Delta V}$$

The combination of high coherence and brightness in a degenerate beam could lead to new applications such as molecular electron holography, using existing diffraction pattern methods, only at a much finer resolution. CNT cathodes themselves are bright, but come short of reaching the limit of quantum degeneracy. However, their brightness can be improved by localization and enhancement of emission by adsorbates on the surface. Certain adsorbates on the emission sites have been shown to dramatically increase brightness, by lowering the field-emission barrier through resonant tunneling between the energy states (Figure 1). In addition to spatially localizing the electron emission, these adsorbates also modify the energy spectrum of emitted electrons [3]. This provides additional scientific motivation, as a way to probe the electronic structure of the adsorbates and their interaction with the surface.

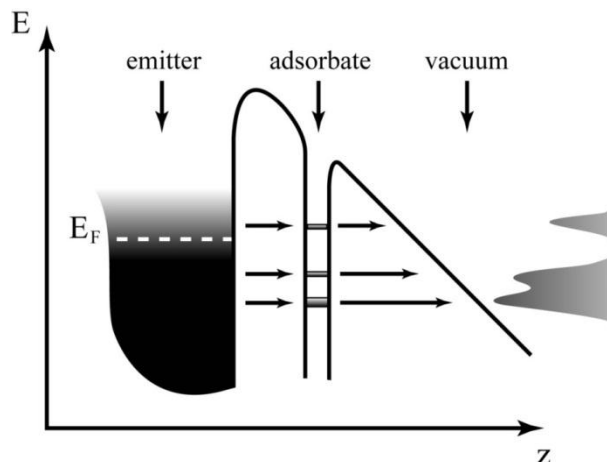


Figure 1 Energy diagram of the emitter-vacuum interface in the presence of an adsorbate and the resulting field emission energy distribution. (J.D.Jarvis)

A lot of previous work supports this research. Hata & Saito have explored field emission from CNTs with adsorbates using field emission microscopy [4], showing that emission current is strongly correlated to adsorbate activity, including changes in binding orientation and location as well as desorption. Reifenberger describes using a retarding mesh spectrometer to measure electron energy spectra [5], and Plummer characterized the effect of adsorbates on the energy spectra of emission from a tungsten surface [3]. In our own lab, Prof. Jarvis has performed extensive work on field emission from diamond field-emitter arrays [2]. His work, measuring spectra of clean diamond field-emitters and of adsorbates on diamond, is what motivated this project. Our goal is to build upon this information by measuring field-emission energy spectra from adsorbates on CNTs, and then find the right adsorbate to allow us to demonstrate a quantum degenerate beam.

3 Experiments

3.1 Cathode Preparation

Initially we used 10-30 nm, catalytically grown multi-wall CNTs purchased from SES Research. However, catalytic CNTs often do not have closed caps, and may still contain the catalyst particle at the end of the tube. Because we are interested in the electronic structure of the cap, catalyst particles could introduce an unknown perturbation, which could affect emission. We switched to using 6-20nm multi-wall CNTs produced through arc discharge, purchased from Materials & Electrochemical Research Company (MER). They are provided in a purified powder form, which is a mixture of tubes and some remaining ash. Arc-discharge tends to produce tubes bundled into small fibers, which we can easily see using a high magnification optical microscope.

We use ultra-sharp tungsten needles as a structural base on which to mount the CNTs. To prepare the needles, we electrochemically etched 100 μm tungsten wire, purchased from Goodfellow Corp., to produce a sharp tip less than 100 nm across. We used a 1 M solution of NaOH as the electrolyte, with a Ni wire cathode and the tungsten wire, submerged 2 mm below the surface, as the anode. A small bias applied between the cathode and anode causes electrolysis to etch away the tungsten. Surface effects cause the etching to proceed most rapidly at the meniscus around the tungsten wire, weakening the wire at the surface until the submerged portion falls off. As the wire is etched away, the resistance between the wire and solution increases, causing the etching current to decrease, until the wire breaks and the current decreases abruptly. We monitor the current using LabView to detect the moment the wire breaks, and switch off the bias to avoid over-etching the tip. The needles are then rinsed in de-ionized water to remove any NaOH crystals.

To mount nanotubes on the needles we use a 3-axis translational stage driven by Picomotors to pick up tubes from a sample under an optical microscope (Figure 2). The needles are attached to a vibration-damped arm attached to the translational stage, which is mounted under the optical microscope and grounded. Nanotube samples are prepared by wrapping conductive carbon tape around the edge of a small piece of aluminum shim stock and lightly touching this edge to loose nanotube powder, then gently tapping to remove loose powder. This sample is mounted on a metal block under the microscope, which is biased using a DC voltage source. Biasing the nanotube sample relative to the needle provides a polarizing effect when near a nanotube, helping achieve better contact while mounting. In addition, monitoring the current between the sample and needle holder indicates contact between the needle and nanotubes, and the stability of the current indicates the stability of the adhesion between the needle and tubes.

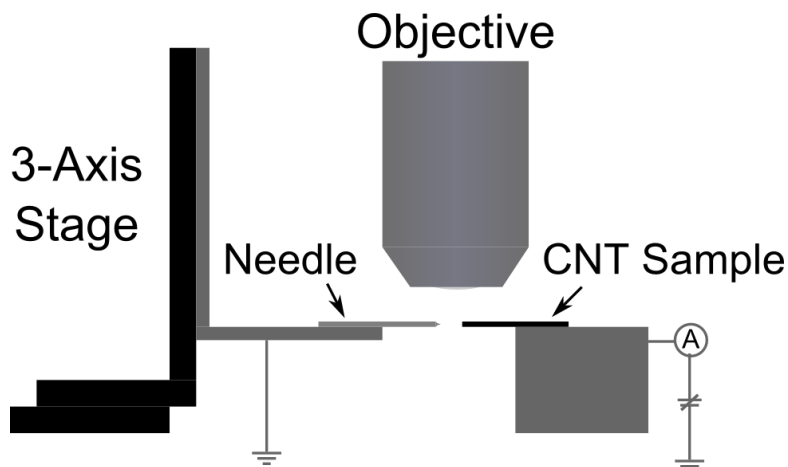


Figure 2 Diagram of CNT mounting apparatus under the optical microscope. A Tungsten needle is attached to the arm of the translational stage, and the nanotube sample is placed on a metal block.

To mount nanotubes on the needle, first we locate a straight, free standing bundle of nanotubes and bring the needle in from the side to overlap most of the visible bundle. Tapping the surface agitates the contact, allowing the tube to settle into a position with good adhesion, indicated by a stable current through the contact area. Pulling the needle away can either pull the bundle apart, leaving a section on the needle with a few individual tubes protruding from the free end (Figure 3a), or pull off a large clump of tubes that the bundle is attached to. In the latter case, the clump can often be separated from the bundle by touching it to a clean section of the carbon tape. Sometimes the bundle separates, and any potential remaining tubes cannot be resolved by the optical microscope, but their presences can be verified by bringing the tip close to another nanotube still on the sample and watching the current to detect electrical contact. Bundles tapering down to single tubes are preferable to a single nanotube on the needle because the larger surface area in contact with the tungsten needle provides increased adhesion and a more rigid cathode, which is more likely to remain aligned.



Figure 3 a) Optical microscope image (1000x) of tungsten needle tip and CNT bundle after mounting procedure. b) SEM image of same specimen, showing the bundle attached to the needle, with a single nanotube protruding from the tip.

Once a nanotube is mounted on the needle, the potential cathode is removed to be imaged in the SEM (Figure 3b). Only then can the individual tubes be resolved to verify that it is a useful cathode. If we find there is a good, axially aligned tube on the tip, we use carbon deposition induced by the focused beam to try to improve adhesion to the needle. Focusing the SEM tightly on the area of overlap between the bundle and the needle and rastering it rapidly across this area causes deposition of carbon contamination in the chamber, forming a “nanoweld” between the CNTs and the needle.

3.2 Cathode Testing and Cleaning

Once the cathodes are imaged they are mounted in the field-emission microscope (FEM) test chamber for cleaning and characterization. The FEM is a simple test system, with a mesh screen anode and phosphor screen, operated at 10^{-10} Torr in a UHV chamber (Figure 4). We spot-weld the needle to another, ‘U’ shaped section of tungsten wire used as a heater filament. This is then mounted on the end of a linear actuator in the UHV chamber. The needle is held at a short distance (~ 1 cm) from the wire mesh anode, which can be varied between 0 kV-5 kV. This extraction field produces the electron beam through field emission from the nanotube, and the electrons are allowed to drift and expand through the mesh anode before striking a phosphor screen on the opposite side. The current on the screen is monitored using a floating, logarithmic ammeter to measure the total cathode current, and the image is recorded using a video camera.

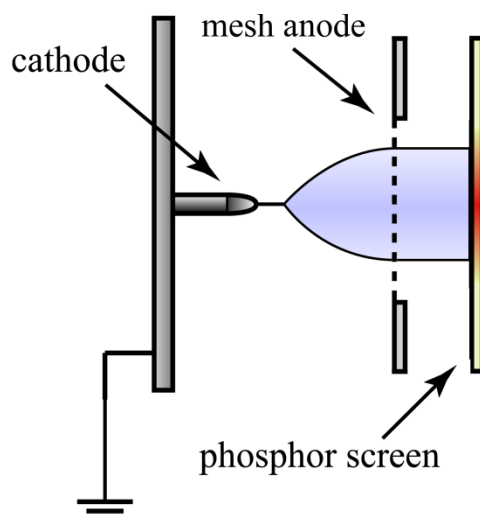


Figure 4 Diagram of Field Emission Microscope, used for testing and cleaning CNT cathodes.

For a good cathode, initial turn-on typically occurs around 500 V. At first the emission current is noisy and the FEM image shows little structure, since the surface is contaminated by residual gases adsorbed to the cap and must be cleaned. The field-emission current excites some of the adsorbates, driving them off or rearranging them on the surface. This often causes the current to begin to rise initially. Further cleaning can be achieved by heating the cathode with the tungsten heater filament. This conductively heats the nanotube, increasing the surface temperature of the cap, providing additional energy to adsorbates, reducing their average lifetime on the surface.

More localized cleaning can be achieved using Joule heating. Resistive heating of the emission sites due to the large currents passing through them provides energy to help remove adsorbates, especially those which enhance the emission current. However, if the emission current is too large, it causes significant outgassing from the phosphor screen, degrading the vacuum, so we pulse the field at a 50% duty factor to reduce the impact on the vacuum. This localized heating can be used in a more targeted manner using “adsorbate-assisted desorption.” Many adsorbates provide local emission enhancement through resonant tunneling, and any polarizable residual gases are more strongly attracted to the emission sites, where the field is strongest due to the field enhancement from the increased curvature. Particularly stubborn adsorbates can often be removed by turning off the heater current and reducing the emission current. After some time, a new adsorbate may bind nearby an existing one, at which point increasing the extraction field causes an enhanced increase in the local emission current, increasing local Joule heating. This can provide enhanced local heating on short time scales, allowing tightly bound adsorbates to be removed on reasonable time scales.

Through cleaning, the structure of the underlying CNT begins to show in the FEM image. A closed cap on a carbon nanotube must have 6 pentagonal rings, at which the surface of the nanotube is

‘puckered’. (Figure 5) Since the higher curvature means a larger field-enhancement factor, emission is strongest from these pentagons, making them the characteristic signature of a clean CNT. The caps are not necessarily symmetrical, and the pentagons can be arranged in many, essentially random ways on the cap [6], although we have found that all 6 pentagonal rings are not always visible. Since they are coherent sources, they will produce interference fringes between adjacent pentagonal rings (Figure 6).

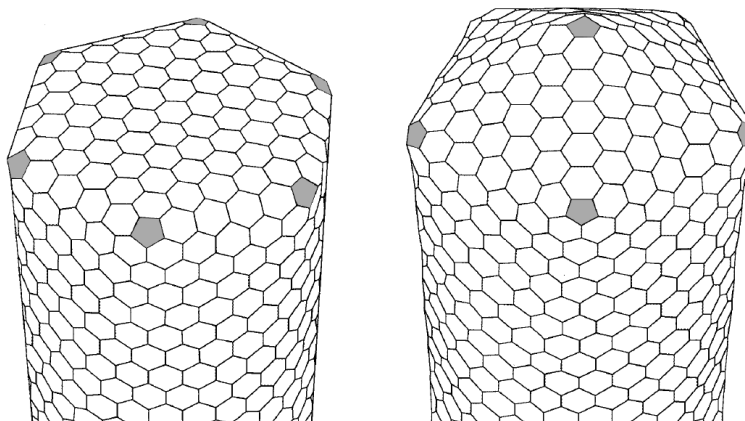


Figure 5 Wire-mesh model of nanotube caps, showing different symmetrical arrangements. [6]

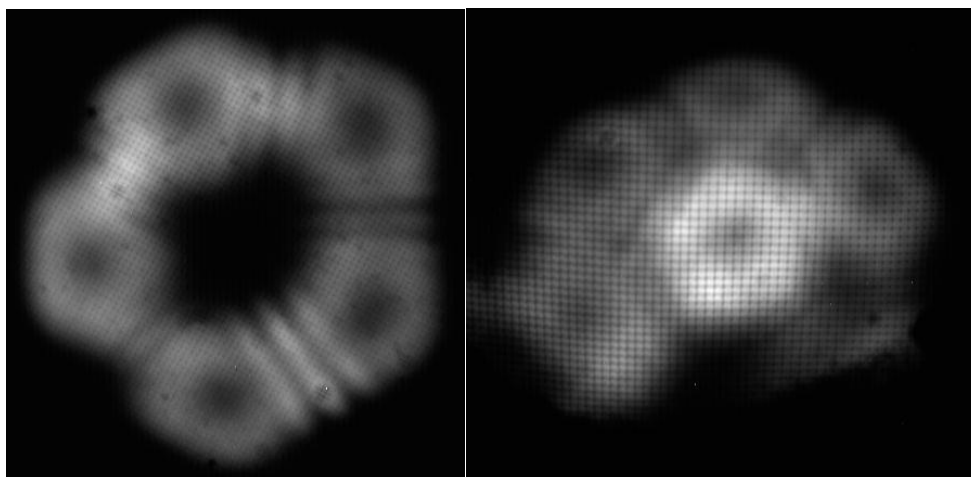


Figure 6 FEM images of clean, closed-cap CNT emission patterns, showing characteristic, coherent emission from pentagonal rings with interference fringes in between.

3.3 Adsorbate Behavior

Once the CNT is clean, we can distinguish the behavior of individual adsorbates on the emission sites. With the heater filament hot, we can demonstrate a stable emission current, with no adsorbate activity over a long time scale. Reducing the surface temperature, by turning down the heater filament or reducing the emission current, allows residual gas molecules to adsorb to the tip. Once captured, the current can be increased to prevent further adsorption.

In order to take advantage of the enhanced brightness from adsorbates, we must find an atom or molecule which binds more tightly to the surface of the tube. To do this we need to be able to selectively

deposit known adsorbates on the surface. If we introduce the desired adsorbate as a vapor at sufficient pressure, we should soon see activity on the surface, and the strong field enhancement factor should increase binding for any polarizable adsorbates. If the vacuum is clean, and the cathode emission has been stable on a long time scale, then essentially all activity following the introduction of the vapor can be assumed to be due to our desired adsorbate.

We tested a range of adsorbates, from random, residual gases remaining in the vacuum chamber to various atomic metal adsorbates and organic molecules. The residual gas molecules were easily adsorbed by reducing the cathode heater and turning off the ion pump to allow the vacuum to degrade slightly. We attempted to develop a calcium vapor source using the decomposition of calcium carbonate on a molybdenum filament, but opted to use commercially available sodium and cesium sources instead. We also experimented with several molecular adsorbates, such as water, carbon dioxide, and acetonitrile, a polar organic molecule. Our initial results reveal that we don't understand the binding process well enough yet, and have more work to do in order to find a suitable adsorbate, but trouble producing reliable cathodes has hindered rapid progress.

3.4 Energy analyzer

We used a custom retarding-potential analyzer to measure the emission spectra of the cathodes (Figure 7). The front face of the analyzer functions as the anode, and is coated with a europium-doped yttrium oxide phosphor powder. An electrostatic deflection system steers the beam to a small aperture, which samples a narrow solid angle. The resulting, roughly collimated beam is focused by another electrode so that the electron trajectories are parallel when they reach the retarding mesh. The mesh bias is swept across a range of a few volts, relative to ground, and electrons with sufficient energy continue through to be collected. The differential change in collector current as the mesh bias is swept gives the energy distribution of the electrons. The resolution of this type of spectrometer is limited by spherical aberration in the focusing lens and field leakage through the finite wire mesh. These effects can be minimized by reducing the anode aperture and using a finer mesh, but at the cost of reducing the collector signal. All measurements reported here were conducted using a 1 mm aperture and a 500 lines/inch mesh, and the collector current was measured by recording the potential difference across a 100 M Ω resistor.

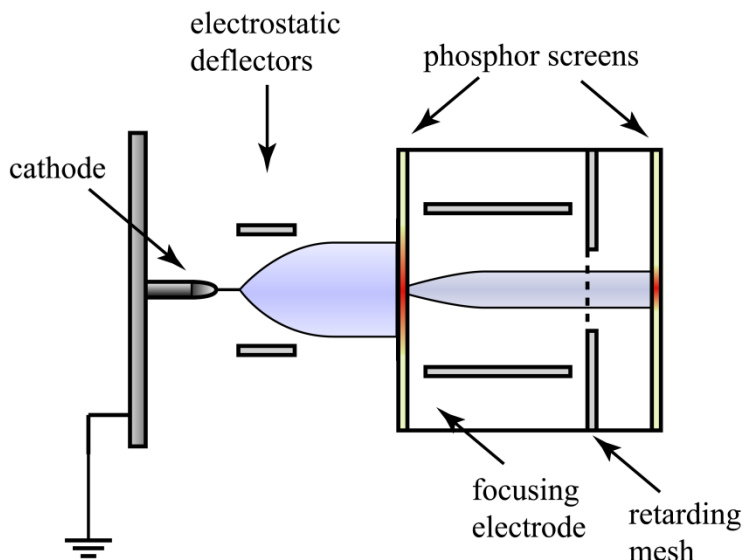


Figure 7 Diagram of retarding mesh energy analyzer used to measure electron energy spectra.

We used simulations run in Simion to estimate the ideal focus voltage, but fine-tuned it by measuring spectral width as a function of the focus voltage (Figure 8). The minimum spectral width should correspond to the electrons trajectories being most nearly normal to the mesh, which is the optimal focusing. We also found that large deflections of the electron beam broaden the spectral width, as the beam strikes the aperture at a larger angle, increasing the effects of spherical aberration.

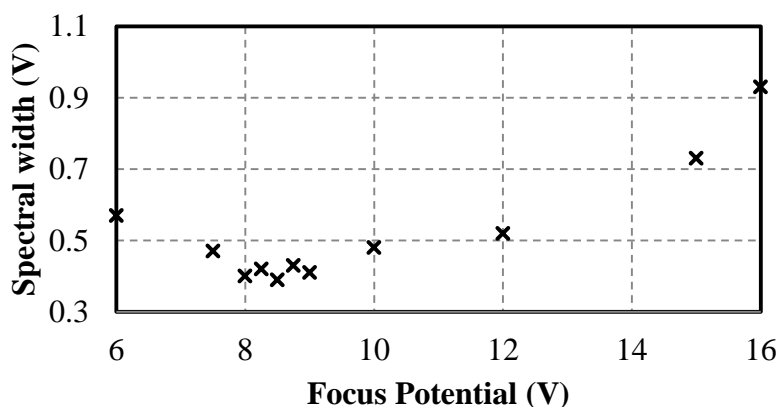


Figure 8 Optimization plot of the full-width half-maximum spectral width measured as a function of the focus potential, with a beam energy of 1 kV. The optimal focus is 8.5 V giving a spectral width of 0.39 V

We used a LaB_6 crystal as a thermionic emitter for calibration. Thermionic emitters have a well-known spectral shape, determined by the Richardson theory, which is depends on the temperature. We used an optical pyrometer to measure the temperature of the tungsten heater filament, and from it

determined the theoretical thermionic emission spectrum. Comparing this to what we measured (Figure 9), and using the deconvolution method developed by Reifenberger [5], we derived the resolution function of the analyzer, and found it had a full-width half-maximum of 0.22 V. This gives us the spectral broadening introduced by the analyzer and the limit of the fine spectral structure that we can resolve.

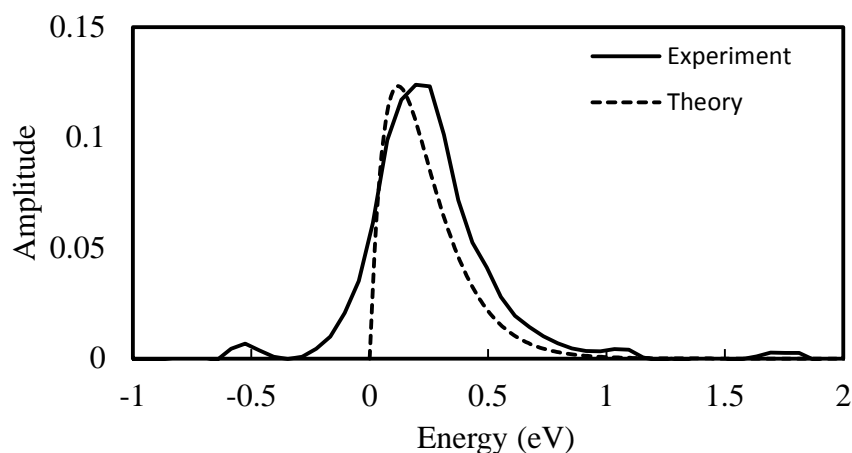


Figure 9 Measured and theoretical energy spectrum from LaB₆ thermionic cathode at 1390 K.

4 Results

Our first significant results after developing the cleaning procedure came from observing various adsorbate events and behaviors on the CNT cap. Once we obtained a clean CNT emission pattern, we could distinguish individual adsorbate events of residual gases and noticed several recurring patterns. These adsorbates could be any of molecular nitrogen, carbon dioxide, water, carbon monoxide, oxygen, etc. Adsorbates preferentially bound to the pentagonal rings on the CNT cap, and would often switch between 5 possible orientations, due to the symmetry. There were several regular structures that often appeared in FEM images, such as a triangle shaped adsorbate, with a relatively bright emission site between two dull emitters (Figure 10) and a common bright, bar shaped structure. It is impossible to identify these adsorbates from the residual gases without a more controlled methodology, but we found that the brighter adsorbates tended to be short lived, likely due to local Joule heating. The behavior of the bar shaped structure, which resembles images of carbon dioxide adsorbates from Hata et al., are of particular interest because they easily rotated around the 5 degenerate orientations. (Figure 11) It is especially interesting that the speed of rotation was clearly correlated with other adsorbate activity, with large nearby emission currents exciting them to rapidly transition between orientations.

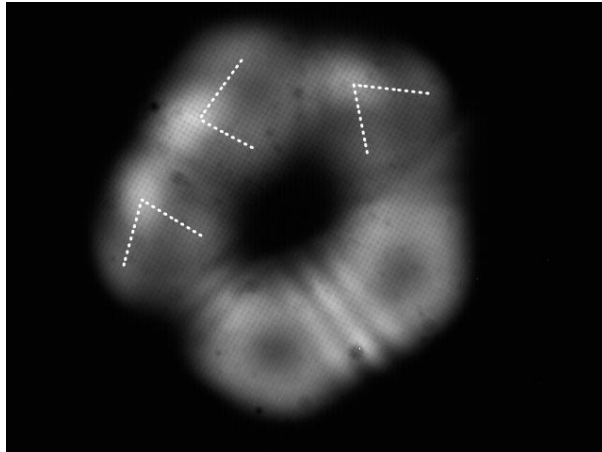


Figure 10 Marked FEM image of triangle adsorbates on clean CNT cap. These unknown adsorbates are stable at high currents, but offer only a small emission enhancement.

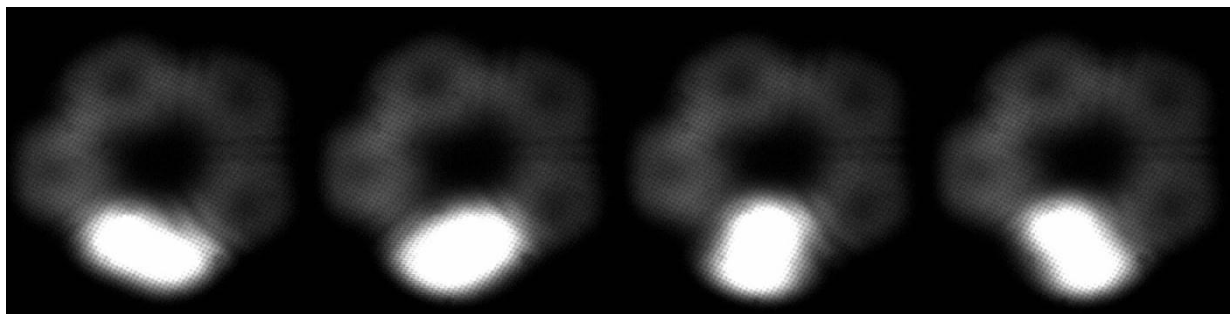


Figure 11 Sequence of FEM images of a bar-shaped adsorbate on a clean CNT cap, showing 4 of the 5 possible orientations on the pentagonal emission sites.

We observed several large emission currents from single adsorbates with short lifetimes. Comparing the total emission current with the adsorbate to the previously stable base emission current, we can estimate the current passing through the adsorbate itself. In one case, we observed an adsorbate with $7 \mu\text{A}$ emission current, which we increased to $10 \mu\text{A}$ by increasing the extraction potential, before the adsorbate was driven off the cathode (Figure 12). Adjusting for the oversaturated FEM image by comparing to similar, unsaturated images, we estimated an RMS size of 2.5 nm for the adsorbate beam spot; and using the geometry and potentials, we estimated the time of flight to be 2.0 ns . Assuming the lateral momentum is constant, this gives a RMS momentum of $1.2 \times 10^{-24} \text{ kg} \cdot \text{m/s}$. Using Equation 1 and assuming a symmetric beam distribution, we estimate a brightness of $B_N = 3.16 \times 10^{18} \frac{\text{A}}{\text{m}^2} \text{sr}$. Estimating 1 V as an upper bound for the energy spread, Equation 2 gives a degeneracy of $\delta = 0.136$, about an order of magnitude below the degeneracy limit of 1.

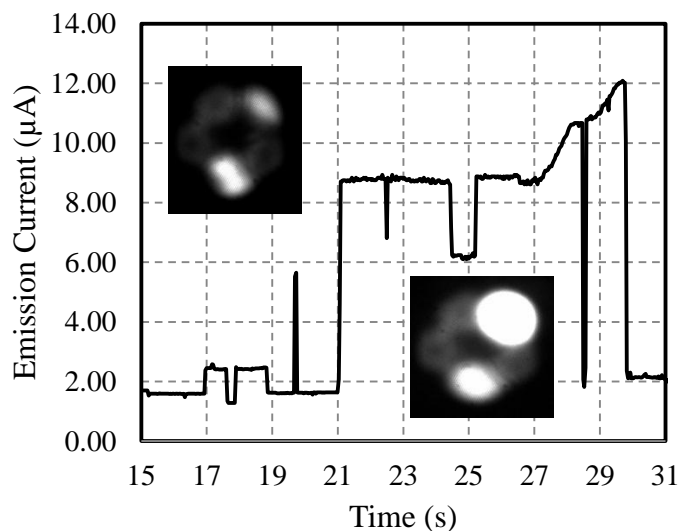


Figure 12 Emission current from single adsorbate event

The results from our custom calcium vapor source were unclear, as there was little assurance the adsorbate activity was due to calcium, and not some other by-product. The commercial sources were more reliable since they included custom getter materials designed to remove all decomposition byproducts. First we tried sodium, and found that we could reliably deposit a single adsorbate on the cap shortly after activating the vapor source, causing increases in emission current of 3-6 μA . These adsorbates had lifetimes up to several minutes with the cathode hot. Following theoretical calculations performed by Joe Driscoll and Prof. Kalman Varga, we chose to test cesium next, as they found it to have a greater binding energy than most alkali metals, with sodium having the least. We would expect to see an exponential increase in lifetime with greater binding energy, however the behavior of cesium adsorbates was not significantly different than that of sodium. This may be because the binding energy is dominated by polarization effects due to the electric field, as further calculations showed that many alkali metals had similar binding energies in the presence of a 0.5 V/\AA electric field.

We hoped to take advantage of the polarization effect by testing molecular adsorbates that are known to be highly polarizable. First we tried bleeding in carbon dioxide, hoping to see a familiar structure to some of the residual gas adsorbates, but unfortunately saw little adsorbate activity. Next we chose to test acetonitrile (CH_3CN), as it is readily available as a liquid which we can easily vaporize and bleed in and also has a strong intrinsic dipole moment. We were able to consistently observe strong activity from these adsorbates, with lifetimes on the order of a minute. Adsorbates could be observed switching between several orientations, but under high extraction field, preferred a specific orientation, which we believe to be with its dipole moment normal to the surface, so that its large aspect ratio shape is aligned with the field, providing an additional field enhancement factor.

Using our calibrated energy spectrometer, we successfully measured the emission spectrum of a clean carbon nanotube, and the emission from an unknown adsorbate on the CNT cap. (Figure 13) The adsorbate's emission spectrum shows a clear change in shape, as expected, due to preferential tunneling from lower-energy, resonant states [3].

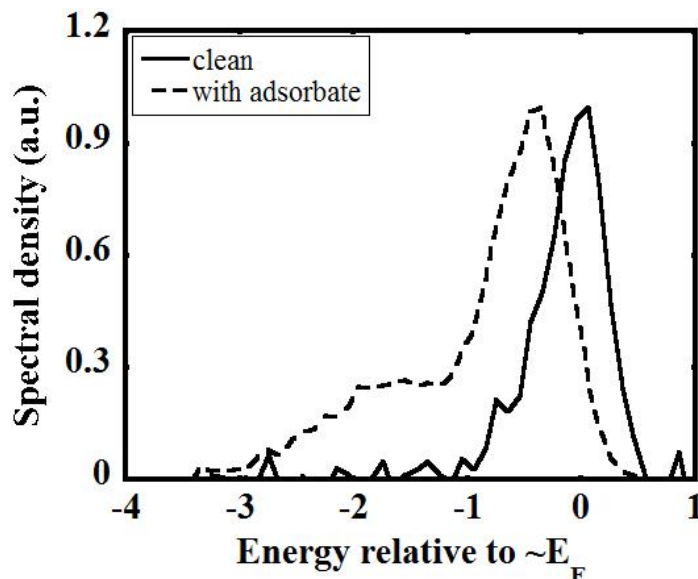


Figure 13 Energy spectra of emission from a CNT, first clean, then with unknown adsorbate.

5 Conclusions and Further Work

We have made progress so far towards achieving a quantum degenerate beam, but need to continue to improve several techniques in order to more reliably produce results. We have encountered the most trouble in producing reliable CNT cathodes. While we have become proficient at mounting CNTs on the etched needles, the success rate of these cathodes is still very low. Most do not survive the initial turn on and cleaning, most likely due to poor adhesion between the tungsten and carbon. We rely on van der Waals forces when initially mounting, then build a 'nanoweld' in the SEM chamber, but this process is clumsy and we are developing a custom nanomanipulator for the SEM which would allow us to perform the mounting in situ. This will give us much greater control in positioning and attaching the CNTs.

Once we can more reliably produce cathodes, we intend to further test a range of adsorbates on the nanotubes. This would include many of the adsorbates we have tested so far, but more reliable cathodes would allow for measurement of the energy spectra as well as emission current. We would like to improve the resolution of the energy analyzer so that we can distinguish the characteristic spectra of these molecules, and characterize how they interact with the surface. Through this we hope to learn what adsorbates have the highest binding energy, and therefore have high lifetimes at high current and would be useful for producing a quantum degenerate beam.

References

- 1 R. H. Fowler and L. Nordheim, Proc. of the Royal Society of London, Series A, Vol. 119, No. 781 (May 1, 1928), pp. 173-181
- 2 J. D. Jarvis, H. L. Andrews, B. Ivanov, C. L. Stewart, N. de Jonge, E. C. Heeres, W.-P. Kang, Y.-M. Wong, J. L. Davidson, and C. A. Brau, J. Appl. Phys. **108**, 094322 (2010)
- 3 E. W. Plummer and R. D. Young, Phys. Rev. B **1**, 2088-2109 (1970)
- 4 K. Hata, A. Takakura, and Y. Saito, Surf. Sci., **490**, 296 (2001).
- 5 R. Reifenberger, H. A. Goldberg, and M. J. G. Lee, Surf. Sci., **83**, 599 (1979).
- 6 Y. Saito, K. Hata, and T. Murata, Jpn. J. Appl. Phys. Vol. 39 (2000), pp. L 271-L 272

Acknowledgements

I would like to thank Prof. Brau for allowing me to undertake this project and providing guidance along the way. I would especially like to thank Prof. Jarvis for patiently teaching me lab procedures and experimental techniques, and most everything else I needed to know for the project. I would also like to thank Prof. Ivanov for his unique insights and always finding any device or chemical we found we needed. Finally, I would like to thank the William A. and Nancy F. McMinn Foundation, whose generous scholarship has supported me during this research and my studies.